

Mass wasting triggered by the 2008 Wenchuan earthquake is greater than orogenic growth

Robert N. Parker¹, Alexander L. Densmore^{1*}, Nicholas J. Rosser¹, Marcello de Michele², Yong Li³, Runqiu Huang³, Siobhan Whadcoat¹ and David N. Petley¹

Shallow earthquakes are the primary driver of rock uplift in mountain ranges¹. However, large shallow earthquakes also trigger widespread, coseismic landslides that cause significant but spatially heterogeneous erosion^{2–4}. The interplay between rock uplift and the distribution and magnitudes of coseismic landslides thus raises a fundamental question as to whether large earthquakes and their associated landslides create or destroy mountainous topography. The 2008 M_w 7.9 Wenchuan earthquake in Sichuan, China triggered more than 56,000 landslides⁵, with a spatial distribution that was only partly related to the pattern of tectonic deformation⁶. Here we examine the potential changes in orogen volume using landslide area–volume scaling relationships^{4,7} applied to high-resolution satellite imagery. We estimate that coseismic landsliding produced $\sim 5\text{--}15\text{ km}^3$ of erodible material, greater than the net volume of $2.6 \pm 1.2\text{ km}^3$ added to the orogen by coseismic rock uplift⁸. This discrepancy indicates that, even if only a fraction of the landslide debris is removed from the orogen over the likely $\sim 2000\text{--}4000\text{ yr}$ earthquake return period⁶, the Wenchuan earthquake will lead to a net material deficit in the Longmen Shan. Our result challenges the widely held notion that large dip-slip or oblique-slip earthquakes build mountainous topography, and invites more careful consideration of the relationships between coseismic slip, mass wasting and relief generation.

It is axiomatic that earthquakes build topography through repeated vertical displacements¹, yet large earthquakes are also a primary trigger of landslides², which play a dominant role in the competition between tectonic and surface processes that drive mountain belt evolution^{9–12}. Recent work^{2–4,7} has shown that landslides are capable of generating sustained high rates of erosion (of the order $1\text{--}10\text{ mm yr}^{-1}$), which poses a challenge to our understanding of how mountainous topography is generated: if the volume of erodible sediment produced by earthquake-triggered landsliding exceeds the coseismically-generated rock volume added to the orogen, then—assuming that this sediment is evacuated from the orogen by other erosional processes—the volume and mean elevation of the orogen must decrease. The relative roles of large earthquakes in generating coseismic rock uplift and facilitating landslide erosion¹³ are thus critical for understanding the balance between crustal advection and denudation.

The M_w 7.9 Wenchuan earthquake of 12 May 2008 in Sichuan Province, China, is ideal for examining the relationships between landsliding and orogen evolution because of its large magnitude, the steep regional topography, and the widespread occurrence of coseismic landsliding^{5,14}. The earthquake occurred

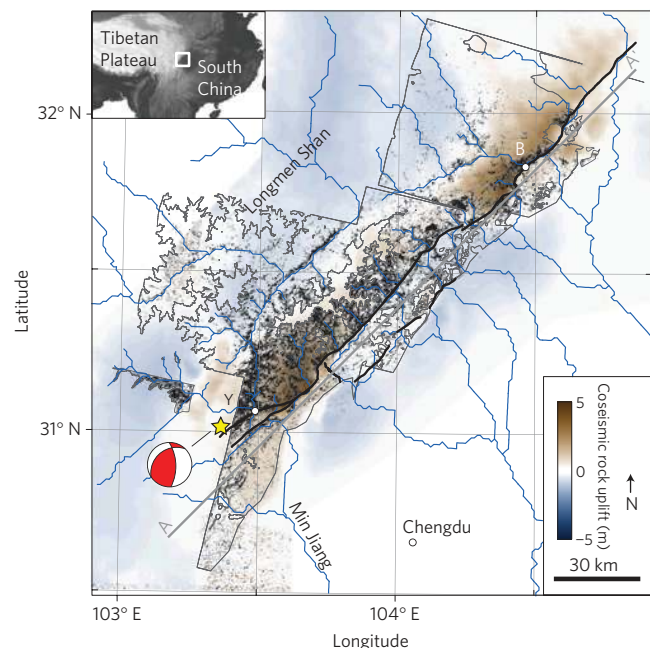


Figure 1 | Coseismic uplift and landslides triggered by the Wenchuan earthquake. Black polygons show individual landslides. Heavy black lines show surface rupture traces¹⁸ and the star indicates the epicentre. Grey outlines show the extent of imagery used in landslide mapping. Background is the coseismic rock uplift field based on SAR analysis, modified from de Michele and colleagues⁸. Heavy grey line shows the rupture-parallel section line onto which the results are projected. Beichuan (B); Yingxiu (Y).

in the Longmen Shan mountain range, which is underlain by a complex lithological assemblage comprising Proterozoic granitic massifs, a Palaeozoic passive margin sequence, a thick Triassic–Eocene(?) foreland basin succession, and minor exposures of poorly-consolidated Cenozoic sediment¹⁵. The faults in the Longmen Shan originated in the Late Triassic¹⁶ and have remained active into the Quaternary as dextral-thrust oblique-slip faults¹⁷. The earthquake involved $>10\text{ m}$ of oblique dextral-thrust surface slip on the Beichuan and Pengguan faults^{6,18} (Fig. 1). Inversion of GPS and InSAR data⁶ coupled with field observations¹⁸ shows that the magnitude and proportion of dextral strike-slip and thrust dip-slip fault displacement varied significantly along the rupture trace, with two distinct zones of concentrated slip and moment release near Yingxiu and Beichuan (Fig. 1).

¹Institute of Hazard, Risk and Resilience and Department of Geography, Durham University, Durham DH1 3LE, UK, ²Bureau de Recherches Géologiques et Minières, Natural Risks Division, 3 avenue Claude Guillemin, 45060 Orléans Cedex 2, France, ³State Key Laboratory of Geohazard Prevention and Geoenvironment Protection, Chengdu University of Technology, Chengdu 610059, Sichuan Province, China. *e-mail: a.l.densmore@dur.ac.uk.

To constrain landslide erosion, coseismic and immediate postseismic landslides were mapped within an area of 13,800 km² in the Longmen Shan using high-resolution satellite imagery collected within 30 days of the earthquake (see Methods). We resampled the raw landslide inventory data into landslide density P_{ls} :

$$P_{ls} = A_{ls}/A_t \quad (1)$$

where A_{ls} is the area of all landslides within a chosen window size A_t (ref. 19). Values of P_{ls} calculated with equation (1) vary from >60% (with $A_t = 1 \text{ km}^2$) near the epicentre to 0% in the low-relief Sichuan Basin (Fig. 1). P_{ls} also varies significantly along strike, with high values along the Min Jiang valley near Yingxiu (Fig. 1) and secondary clusters to the northeast, particularly associated with major transverse river valleys. This partly, but not fully, reflects along-strike variations in surface rupture¹⁸. Strong variations in P_{ls} between different lithologies were noted by Dai *et al.*⁵, along with complex relationships between P_{ls} and the distance from the earthquake source. Given that landslide occurrence is not solely tied to coseismic deformation, there is potential for mismatch between patterns and volumes of tectonic rock uplift and landslide erosion.

Understanding the balance between tectonic and mass wasting processes in the Wenchuan earthquake requires a scaling relationship to convert individual landslide area A_i to total volume V_{ls} :

$$V_{ls} = \sum_1^n \alpha A_i^\gamma \quad (2)$$

where n is the number of landslides and the scaling parameters α and γ are constants that vary with setting and hillslope process (for example bedrock or shallow landslides). We applied equation (2) using published scaling parameters^{4,7} as well as those derived from field measurement of 41 landslides in the study area. The results (Table 1) are strikingly consistent and place first-order constraints on the likely volume of material involved. Application of a global best-fit relationship for all landslide types from Larsen *et al.*⁴ with $\gamma = 1.332 \pm 0.005$ yields $V_{ls} = 5.73 + 0.41/\gamma - 0.38 \text{ km}^3$. A global best-fit relationship for bedrock landslides from Larsen *et al.*⁴ ($\gamma = 1.35 \pm 0.01$) and a relationship derived from field measurements ($\gamma = 1.388 \pm 0.087$) both yield similar values of $V_{ls} \approx 9 \text{ km}^3$, whereas a global relationship from Guzzetti *et al.*⁷ yields $V_{ls} = 15.2 + 2.0/\gamma - 1.8 \text{ km}^3$. The predicted volumes in Table 1 are minima, because the images span most but not all of the surface rupture (see Methods), but are consistent with spatially-averaged denudation of 0.42–1.1 m over the 13,800 km² mapped area. Conversion of these estimates to landslide erosion rates requires knowledge of the recurrence intervals of large landslide-triggering earthquakes on the Beichuan fault, but these are poorly constrained by limited dating at a few widely-spaced trench sites^{20,21} or inferred rates of strain

accumulation⁶. Assuming plausible recurrence intervals of 2,000–4,000 yr (refs 6,20) yields a long-term, spatially-averaged erosion rate due to landsliding alone of 0.1–0.6 mm yr⁻¹, similar to the pre-earthquake total erosion rates of 0.2–0.6 mm yr⁻¹ in the eastern Longmen Shan estimated from cosmogenic nuclide analyses over similar millennial timescales²².

These landslide volume estimates can be compared with the volume of material added to the orogen in the earthquake through coseismic rock uplift. de Michele *et al.*⁸ inverted ascending and descending mode Synthetic Aperture Radar (SAR) data (see Methods) to obtain the three-dimensional surface displacement vectors at ~350 m intervals across the region (Fig. 1). We sum the vertical component of these data (equation (3)) over the area of our landslide mapping to obtain a net positive volume gain $V_t = 2.6 \pm 1.2 \text{ km}^3$. This is more than one standard error less than all estimates of landslide volume (Table 1), and implies that the earthquake added much less volume to the Longmen Shan than was potentially released by landsliding (Fig. 2). There are, however, two important caveats to this direct comparison. First, the SAR data were obtained between November 2006 and August 2008, and thus record surface change due to coseismic and postseismic landslides as well as coseismic and postseismic deformation. Landsliding affects only about 4% of the 13,800 km² mapped area, however, minimizing the effect of landsliding on V_t . Also, disruption of the ground surface by landsliding causes local incoherence in the SAR analysis, and incoherent pixels are not used in the calculation of surface displacements⁸. The displacement magnitudes and directions determined from the inversion closely match field observations^{8,18}, suggesting that at the orogen scale the displacement estimates are not strongly biased by landslide-induced surface change. Second, and more significantly, estimated landslide volume does not necessarily equate to eroded volume; conversion to an orogen-scale erosion rate requires that the landslide debris be efficiently flushed from the orogen¹³. Although there was some sediment storage along major Longmen Shan river valleys before the earthquake, the overall preponderance of bare-bedrock hillslopes and general lack of thick (>100 m) sediment stores^{22,23} suggest that coseismic landslide debris is likely to be efficiently removed over the entire earthquake cycle, but the lack of pre- and post-earthquake sediment discharge data prevents us from quantifying the rate of removal^{13,24}.

Thus, if hillslope and fluvial processes can remove the Wenchuan landslide debris before the next large landslide-triggering earthquake, then the earthquake will likely have caused a significant net volume loss from the orogen. How does this imbalance affect the growth of topography in the Longmen Shan? We stress that our results are an instantaneous measure of the competition between erosional and tectonic processes and bear only indirectly on the long-term volumetric balance that defines an orogen¹¹. It is possible that the range is in topographic decay, as suggested by Godard *et al.*²⁵, with rates of erosion outpacing those of rock uplift,

Table 1 | Landslide scaling relationships and volume estimates.

Relationship*	α	γ	Volume [†] (km ³)	Mean erosion (m) [‡]	Erosion rate (mm yr ⁻¹) [§]	Reference
L1 (all landslides)	0.146	1.332 ± 0.005	5.73 + 0.41/γ - 0.38	0.42	0.1–0.2	4
L2 (all bedrock landslides)	0.186	1.35 ± 0.01	9.36 + 1.39/γ - 1.21	0.68	0.2–0.3	4
L3 (mixed Himalayan landslides)	0.257	1.36 ± 0.01	14.9 + 2.2/γ - 1.9	1.1	0.3–0.5	4
G (all landslides)	0.074	1.450 ± 0.009	15.2 + 2.0/γ - 1.8	1.1	0.3–0.6	7
Field measurements	0.106	1.388 ± 0.087	9.08 + 22.2/γ - 6.35	0.66	0.2–0.3	This study

*L1: global relationship for all landslides from Larsen *et al.*⁴; L2: global relationship for all bedrock landslides from Larsen *et al.*⁴; L3: relationship for mixed bedrock and soil landslides in the Himalaya from Larsen *et al.*⁴; G: global relationship for all landslides from Guzzetti *et al.*⁷. [†]Uncertainties are expressed by applying equation (2) with ±1 s.d. error on γ . [‡]Mean erosion represents the average lowering of the ground surface due to landsliding and is calculated by dividing the estimated volume by the total study area (A_{map}). [§]Spatially-averaged landslide erosion rate is determined by dividing mean erosion range by the approximate earthquake recurrence interval of 2,000–4,000 yr (refs 6,20).

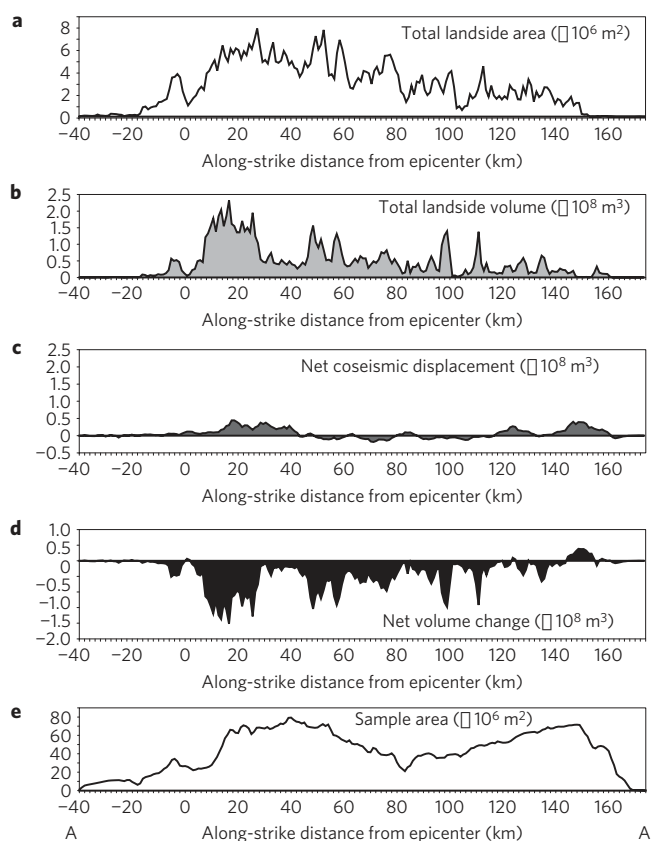


Figure 2 | Along-strike variations in landslide occurrence and coseismic displacement. All data are projected onto a rupture-parallel line A–A' (Fig. 1) at 1 km intervals. **a**, Total area of landslides within each 1-km wide strip. **b**, Landslide volume derived from the global bedrock landslide scaling relationship⁴ applied to individual landslides within each 1-km wide strip; other relationships show similar patterns. **c**, Net coseismic volume change⁸ in each 1-km wide strip. **d**, Net volume change determined by subtracting landslide volumes from coseismic volume change. **e**, Along-strike distribution of sample area covered by satellite imagery. Local minima in landslide area and volume are not correlated with small sample areas.

although this model remains to be tested through more focused thermochronological investigation. A second possibility is that some of the long-term rock uplift is accumulated through interseismic deformation²⁶ or afterslip^{27,28}, although the latter mechanism in particular has tended to yield a small fraction of the coseismic displacement. Alternatively, an important fraction of long-term rock uplift may occur in more frequent smaller, or deeper, earthquakes that generate lower peak ground acceleration values²⁹ and trigger a much lower volume of landslides^{2,3}. In that scenario, large or shallow earthquakes would serve primarily to reduce the tectonic topography constructed by smaller or deeper earthquakes and maintain hillslopes at threshold gradients. In support of this idea, Ouimet³⁰ noted that short-term (10^3 yr) erosion rates in the Longmen Shan are $0.2\text{--}0.3\text{ mm yr}^{-1}$, lower than rates over Myr timescales ($0.5\text{--}0.7\text{ mm yr}^{-1}$; ref. 25), and suggested that large earthquakes allow erosion rates to catch up with longer-term rock uplift rates. Climatic conditions will also probably play a role in determining the precise pattern and volume of landslides in response to a given earthquake; given the order-of-magnitude agreement between our estimated rates of landslide erosion and both long- and short-term regional erosion rates, however, temporal variations in climate are unlikely to exert significant changes on the volume balance. A further possibility is that the balance between rock uplift and landslide erosion in the Wenchuan earthquake was anomalous and cannot

be extrapolated over multiple earthquake cycles. It seems likely that earthquakes with a larger component of shortening will lead to a net addition of rock volume, whereas dominantly strike-slip events will cause a net loss due to widespread landsliding but limited rock uplift. Dextral and thrust slip in the Wenchuan earthquake were highly partitioned between different fault strands¹⁸, and the ratio of rock uplift to lateral slip on those strands may vary between earthquakes¹⁷. Large differences in that ratio in successive earthquakes would thus be expected to yield major temporal variations in the net volume balance, even if the pattern and total volume of landsliding remained the same. In any case, the apparent and provocative mismatch between tectonic and erosional volumes involved in the Wenchuan earthquake points to a need for much greater understanding of the role of large earthquakes in setting regional erosion rates and long-term patterns of orogen evolution.

Methods

Landslide mapping. We developed a semi-automated detection algorithm using EO-1 and SPOT 5 imagery for objective mapping of individual landslides (see Supplementary Information). Landslide areas were extracted from EO-1 imagery using an intensity threshold and a 20° gradient mask to remove false positives in valley floors; independent work⁵ shows that areas with a gradient of $<20^\circ$ have very low landslide densities. Unsupervised classification with a 20° gradient mask was used to delineate landslide areas in SPOT 5 imagery. A series of feature-oriented filters were applied to remove false positives produced by roads and fields, and the map was visually inspected and corrected. This resulted in a landslide map with a total area of $13,800\text{ km}^2$ (Fig. 1) that covers 150 km of the 225 km surface rupture^{6,18}, so that the total landslide area and volume calculated here are minimum values. Comparisons with field evidence¹⁸, fault models⁶, and SAR analysis⁸, and with independent landslide maps compiled by hand from imagery and aerial photographs⁵, however, suggest that the mapped area covers the majority of coseismic slip and represents a significant sample of the main impact zone of the earthquake.

Coseismic volume estimation. By combining C- and L-band space-borne SAR amplitude data, de Michele *et al.*⁸ derived the three-component coseismic surface displacement field due to the Wenchuan earthquake. Here we used the up, or vertical, component to calculate the net coseismic volume change in the Longmen Shan, ignoring elevation change in the low-relief Sichuan Basin (Fig. 1). Within the area of the Longmen Shan covered by the landslide mapping (Fig. 1), we calculated the net volume change as

$$V_t = A \sum_{x=1}^n U_x \quad (3)$$

where A is the cell area, U_x is the vertical displacement for each cell, and n is the number of cells, yielding $V_t = 2.6 \times 10^9\text{ m}^3$. The standard deviation of the difference between the displacements and ground truth data is not a good statistical indicator of the uncertainty in V_t , because random (uncorrelated) errors are likely to lead to a negligible net contribution to the total volume over the mapped area. Instead, we estimated the uncertainty in V_t by evaluating the magnitude of statistical variation in U_x within a non-deforming area far from the earthquake rupture. We chose a $36\text{ km} \times 36\text{ km}$ area in the Sichuan basin, 45 km away from the fault rupture, containing a high level of noise (mean of 0 m and standard deviation of 1.5 m). We extracted 30 profiles, each 36 km long, within the selected area, and used the least squares method to fit each profile by linear regression. Because the y -intercept value influences the volume estimation beneath each $36\text{ km} \times 1\text{ pixel}$ area, we examined the y -intercept parameter for each of the profiles and calculated the Root Mean Square Error (RMSE) between the 30 y -intercept parameters and the ground truth data. This yields an RMSE of 0.10 m; when applied over the entire mapped area, this is equivalent to an estimated uncertainty of $1.2 \times 10^9\text{ m}^3$ on V_t .

Received 4 November 2010; accepted 15 April 2011;
published online 15 May 2011

References

- Avouac, J. P. in *Crustal and Lithosphere Dynamics* (ed. Watts, A. B.) 377–439 (Treatise on Geophysics, Vol. 6, Elsevier, 2008).
- Keefer, D. K. The importance of earthquake-induced landslides to long-term slope erosion and slope-failure hazards in seismically active regions. *Geomorphology* **10**, 265–284 (1994).
- Malamud, B. D., Turcotte, D. L., Guzzetti, F. & Reichenbach, P. Landslides, earthquakes and erosion. *Earth Planet. Sci. Lett.* **229**, 45–59 (2004).
- Larsen, I. J., Montgomery, D. R. & Korup, O. Landslide erosion caused by hillslope material. *Nature Geosci.* **3**, 247–251 (2010).

5. Dai, F. C. *et al.* Spatial distribution of landslides triggered by the 2008 M_s 8.0 Wenchuan earthquake, China. *J. Asian Earth Sci.* **40**, 883–895 (2011).
6. Shen, Z. K. *et al.* Slip maxima at fault junctions and rupturing of barriers during the 2008 Wenchuan earthquake. *Nature Geosci.* **2**, 718–724 (2009).
7. Guzzetti, F., Ardizzone, F., Cardinali, M., Rossi, M. & Valigi, D. Landslide volumes and landslide mobilization rates in Umbria, central Italy. *Earth Planet. Sci. Lett.* **279**, 222–229 (2009).
8. de Michele, M., Raucoules, D., de Sigoyer, J., Pubellier, M. & Chamot-Rooke, N. Three-dimensional surface displacement of the 2008 May 12 Sichuan earthquake (China) derived from Synthetic Aperture Radar: Evidence for rupture on a blind thrust. *Geophys. J. Int.* **183**, 1097–1103 (2010).
9. Hovius, N., Stark, C. & Allen, P. Sediment flux from a mountain belt derived by landslide mapping. *Geology* **25**, 231–234 (1997).
10. Densmore, A. L., Ellis, M. A. & Anderson, R. S. Landsliding and the evolution of normal fault-bounded mountains. *J. Geophys. Res.* **103**, 15203–15219 (1998).
11. Whipple, K. X. The influence of climate on the tectonic evolution of mountain belts. *Nature Geosci.* **2**, 97–104 (2009).
12. Hovius, N., Stark, C. P., Chu, H. T. & Lin, J. C. Supply and removal of sediment in a landslide-dominated mountain belt: Central Range, Taiwan. *J. Geol.* **108**, 73–89 (2000).
13. Hovius, N. *et al.* Prolonged seismically induced erosion and the mass balance of a large earthquake. *Earth Planet. Sci. Lett.* **304**, 347–355 (2011).
14. Sato, H. P. & Harp, E. L. Interpretation of earthquake-induced landslides triggered by the 12 May 2008, $M_7.9$ Wenchuan earthquake in the Beichuan area, Sichuan Province, China using satellite imagery and Google Earth. *Landslides* **6**, 153–159 (2009).
15. Burchfiel, B. C., Chen, Z., Liu, Y. & Royden, L. Tectonics of the Longmen Shan and adjacent regions. *Int. Geol. Rev.* **37**, 661–735 (1995).
16. Li, Y., Allen, P. A., Densmore, A. L. & Qiang, X. Evolution of the Longmen Shan Foreland Basin (Western Sichuan, China) during the Late Triassic Indosinian Orogeny. *Basin Res.* **15**, 117–138 (2003).
17. Densmore, A. L. *et al.* Active tectonics of the Beichuan and Pengguan faults at the eastern margin of the Tibetan Plateau. *Tectonics* **26**, TC4005 (2007).
18. Liu-Zeng, J. *et al.* Coseismic ruptures of the 12 May 2008, M_s 8.0 Wenchuan earthquake, Sichuan: East–west crustal shortening on oblique, parallel thrusts along the eastern edge of Tibet. *Earth Planet. Sci. Lett.* **286**, 355–370 (2009).
19. Meunier, P., Hovius, N. & Haines, J. Regional patterns of earthquake-triggered landslides and their relation to ground motion. *Geophys. Res. Lett.* **34**, L20408 (2007).
20. Ran, Y. *et al.* Paleoseismic evidence and repeat time of large earthquakes at three sites along the Longmenshan fault zone. *Tectonophysics* **491**, 141–153 (2010).
21. Lin, A., Ren, Z., Jia, D. & Miyairi, Y. Evidence for a Tang–Song dynasty great earthquake along the Longmen Shan Thrust Belt before the 2008 M_w 7.9 Wenchuan earthquake, China. *J. Seismol.* **14**, 615–628 (2010).
22. Ouimet, W. B., Whipple, K. X. & Granger, D. E. Beyond threshold hillslopes: Channel adjustment to base-level fall in tectonically active mountain ranges. *Geology* **37**, 579–582 (2009).
23. Kirby, E., Whipple, K. X., Tang, W. & Chen, Z. Distribution of active rock uplift along the eastern margin of the Tibetan Plateau: Inferences from bedrock channel longitudinal profiles. *J. Geophys. Res.* **108**, 2217 (2003).
24. Dadson, S. J. *et al.* Earthquake-triggered increase in sediment delivery from an active mountain belt. *Geology* **32**, 733–736 (2004).
25. Godard, V. *et al.* Late Cenozoic evolution of the central Longmen Shan, eastern Tibet: Insight from (U–Th)/He thermochronometry. *Tectonics* **28**, TC5009 (2009).
26. Perfettini, H. *et al.* Seismic and aseismic slip on the Central Peru megathrust. *Nature* **465**, 78–81 (2010).
27. Freed, A. M., Bürgmann, R., Calais, E., Freymueller, J. & Hreinsdóttir, S. Implications of deformation following the 2002 Denali, Alaska, earthquake for postseismic relaxation processes and lithospheric rheology. *J. Geophys. Res.* **111**, B01401 (2006).
28. Hsu, Y. J. *et al.* Frictional afterslip following the 2005 Nias–Simeulue earthquake, Sumatra. *Science* **312**, 1921–1926 (2006).
29. Orphal, D. L. & Lahoud, J. A. Prediction of peak ground motion from earthquakes. *Bull. Seismol. Soc. Am.* **64**, 1563–1574 (1974).
30. Ouimet, W. B. Landslides associated with the May 12, 2008 Wenchuan earthquake: Implications for the erosion and tectonic evolution of the Longmen Shan. *Tectonophysics* **491**, 244–252 (2010).

Acknowledgements

Funding for this research was provided by NERC grant NE/G002665/1, National Natural Science Foundation of China grant 40841010, and the Willis Research Network. M.d.M. was supported by BRGM Research Direction. We thank N. Cox, T. Dewez, N. Hovius, B. Malamud, P. Meunier, D. Milledge, D. Raucoules, R. Schultz, H. Tomlinson, O. Tomlinson, Z. Yan and Y. Zhang for assistance.

Author contributions

R.N.P. and S.W. conducted the landslide mapping and analysis. A.L.D., S.W., Y.L., R.H. and D.N.P. collected field data on the rupture and landslide characteristics. M.d.M. derived the tectonic mass flux. A.L.D. conceived the idea and wrote the paper with input from R.N.P., N.J.R., D.N.P. and M.d.M.

Additional information

The authors declare no competing financial interests. Supplementary information accompanies this paper on www.nature.com/naturegeoscience. Reprints and permissions information is available online at <http://www.nature.com/reprints>. Correspondence and requests for materials should be addressed to A.L.D.